Paramagnon-induced dispersion anomalies in the cuprates

R. S. Markiewicz, S. Sahrakorpi, and A. Bansil
Physics Department, Northeastern University, Boston, Massachusetts 02115, USA
(Received 21 December 2006; revised manuscript received 17 September 2007; published 16 November 2007)

We report the self-energy associated with random-phase approximation magnetic susceptibility in the hole-doped $Bi_2Sr_2CuO_6$ (Bi2201) and the electron-doped $Nd_{2-x}Ce_xCuO_4$ (NCCO) in the overdoped regime within the framework of a one-band Hubbard model. A strong weight is found in the magnetic spectrum around $(\pi,0)$ at about 360 meV in Bi2201 and 640 meV in NCCO, which yields dispersion anomalies in accord with the recently observed "waterfall" effects in the cuprates.

DOI: 10.1103/PhysRevB.76.174514 PACS number(s): 71.38.Cn, 71.45.Gm, 74.72.−h, 79.60.−i

I. INTRODUCTION

Very recent angle-resolved photoemission spectroscopy (ARPES) experiments in the cuprates have revealed the presence of an intermediate energy scale in the 300–800 meV range where spectral peaks disperse and broaden rapidly with momentum, giving this anomalous dispersion the appearance of a "waterfall."[1–6] Similar self-energies have also been adduced from optical data.[7] This new energy scale is to be contrasted with the well-known low-energy "kinks" in the 50–70 meV range, which have been discussed frequently in the cuprates as arising from the bosonic coupling of the electronic system with either phonons[8] and/or magnetic modes.[9] Although low-energy plasmons[10,11] are an obvious choice for the new boson, analysis indicates that the plasmons lie at too high an energy of ~1 eV to constitute a viable candidate.[12] Further, ARPES finds transitions due to other bands only at energies $\geqslant$0.9 eV.[3,13] Here, we demonstrate that paramagnons provide not only an explanation of the energy scale but also of the other observed characteristics of the waterfall effect in both hole- and electron-doped cuprates.

II. MAGNON SELF-ENERGY

A. Generalized self-consistent Born approximation

For this purpose, we have evaluated the self-energy associated with the random-phase approximation (RPA) magnetic susceptibility in the hole-doped $Bi_2Sr_2CuO_6$ (Bi2201) and the electron-doped $Nd_{2-x}Ce_xCuO_4$ (NCCO).[14] In order to keep the computations manageable, the treatment is restricted to the overdoped systems where magnetic instabilities are not expected to present a complication. Our analysis proceeds within the framework of the one-band Hubbard Hamiltonian, where the bare band is fitted to the tight-binding local-density approximation (LDA) dispersion.[15,16] We incorporate self-consistency by calculating the self-energy and susceptibility using an approximate renormalized one-particle Green function

$$G = \bar{Z}/(\omega - \bar{\xi}_k + i\delta), \tag{1}$$

where $\bar{\xi}_k = \bar{Z}(\epsilon_k - \mu)$. Here, ϵ_k are bare energies and μ is the chemical potential, and the renormalization factor is $\bar{Z} \sim (1 - \partial\Sigma'/\partial\omega)^{-1} < 1$. The associated magnetic susceptibility is

$$\chi_0(\vec{q},\omega) = -\bar{Z}^2 \sum_{\vec{k}} \frac{\bar{f}_{\vec{k}} - \bar{f}_{\vec{k}+\vec{q}}}{\bar{\epsilon}_{\vec{k}} - \bar{\epsilon}_{\vec{k}+\vec{q}} + \omega + i\delta}, \tag{2}$$

where δ is a positive infinitesimal $\bar{f}_{\vec{k}} \equiv f(\bar{\epsilon}_{\vec{k}})$ is the Fermi function. The RPA susceptibility is given by

$$\chi(\vec{q},\omega) = \frac{\chi_0(\vec{q},\omega)}{1 - U\chi_0(\vec{q},\omega)}, \tag{3}$$

with U denoting the Hubbard parameter. The self-energy can be obtained straightforwardly from the susceptibility via the expression[17] (at $T=0$)

$$\Sigma(\vec{k},\omega) = \frac{3}{2}\bar{Z}U^2 \sum_{\vec{q}} \int_0^\infty \frac{d\omega'}{\pi} \operatorname{Im}\chi(\vec{q},\omega') \times \left[\frac{\bar{f}_{\vec{k}-\vec{q}}}{\omega - \bar{\xi}_{\vec{k}-\vec{q}} + \omega'} + \frac{1 - \bar{f}_{\vec{k}-\vec{q}}}{\omega - \bar{\xi}_{\vec{k}-\vec{q}} - \omega'} \right]. \tag{4}$$

Concerning technical details, we note that for the generic purposes of this study, all computations in this paper employ a fixed value $\bar{Z}=0.5$, which is representative of the band dispersions observed experimentally in hole- and electron-doped cuprates.[18] Self-consistency is then achieved approximately[19,20] by determining the values of the chemical potential μ and the Hubbard parameter U to keep a fixed doping level and to ensure that the bands are indeed renormalized by the average factor $\bar{Z}=0.5$. The procedure is relatively simple, but it should capture the essential physics of the electron-paramagnon interaction, although our treatment neglects the energy[21] and momentum dependencies of $\bar{Z}$. Note also that in the overdoped regime considered, the effective U values in Bi2201 and NCCO are small enough that the system remains paramagnetic and the complications of the antiferromagnetic instability are circumvented. Specifically, the presented results on Bi2201 are for $x=0.27$ with $\mu = -0.43$ eV and $U=3.2t$, while for NCCO, $x=-0.25$ with $\mu = 0.18$ eV and $U=4t$.

B. Hole doping

Figure 1 summarizes the results for Bi2201. We consider Figs. 1(a) and 1(b) first, which give the real and imaginary parts of the self-energy at several different momenta as a

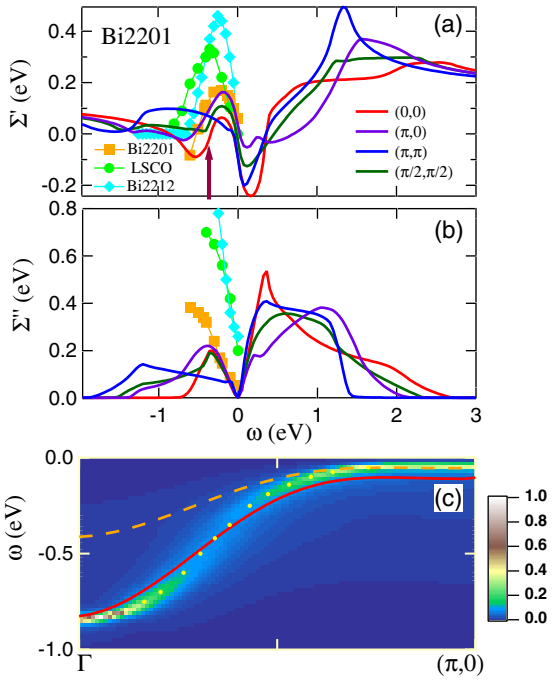

FIG. 1. (Color online) (a) Real and (b) imaginary parts Σ' and Σ'', respectively, of the paramagnon self-energy in overdoped Bi2201. Theoretical results at various momenta are shown by lines of different colors. The values of Σ' have been shifted by a constant to produce a zero average value of the theoretical Σ' at the Fermi level (Ref. 23). Experimental points are from the nodal point for Bi2201 (gold squares, Ref. 3), LSCO (circles, Ref. 5), and Bi2212 (diamonds, Ref. 4). Thin lines joining experimental points are guides for the eye. The arrow marks the location of the peak in χ'' at $(\pi,0)$. (c) Spectral density in the energy-momentum plane obtained from the dressed Green function is shown in a color plot along with the bare (red line) and the renormalized (dashed orange line) dispersions. Dots mark the peak positions of the MDC plots of the dressed spectral density.

function of frequency. The theoretical self-energies, which refer to Bi2201, should be compared directly with the corresponding experimental data (gold squares[3]), although available experimental points for Bi2212 (Ref. 4) and $La_{2-x}Sr_xCuO_4$ (LSCO) (Ref. 5) are also included for completeness. The agreement between theory and experiment is seen to be quite good for the real part of the self-energy in Fig. 1(a), while theory underestimates the imaginary part of the self-energy by a factor of ~2. That the computed Σ'' is smaller than the experimental one is to be generally expected, since our calculations do not account for scattering effects beyond those of the paramagnons. Here, we should keep in mind that there are uncertainties inherent in the experimental self-energies due to different assumptions invoked by various authors concerning the bare dispersions in analyzing the data. In particular, Xie *et al.*[4] extracted the bare dispersion by assuming that Σ' is always positive and goes to zero at large energies. Other groups[3,22] compared their results to LDA calculations and argued that Σ' must become negative at higher energies. Our computed Σ' in Fig. 1(a) becomes negative over the range 0.35–0.9 eV in certain $\vec{k}$ directions.[23] Interestingly, various computed colored lines in Figs. 1(a) and 1(b) more or less fall on top of one another, indicating that the self-energy is relatively insensitive to momentum, especially below the Fermi level, consistent with experimental findings,[5] even though Σ possesses a fairly strong frequency dependence.

Figure 1(c) gives further insight into the nature of the spectral intensity obtained from the self-energy of Eq. (4). The spectral intensity shown in the color plot of the figure is representative of the ARPES spectrum, matrix element effects[24] notwithstanding. The peak of the spectral density function defined by taking momentum density cuts (MDCs), shown by yellow dots, follows the renormalized dispersion (orange dashed line) up to binding energy of about 200 meV. It then disperses to higher energies rapidly (waterfall effect) as it catches up with the bare dispersion (red solid line) around Γ. In fact, near Γ, the dressed spectral peak lies slightly below the bare band. The width of the spectral function is largest in the intermediate energy range of 200–600 meV, where its slope also is the largest. This behavior of the spectral function results from the presence of peaks in the real and imaginary parts of the self-energy in the 200–500 meV energy range discussed in connections with Figs. 1(a) and 1(b) above. It is also in accord with the waterfall effect observed in ARPES experiments, although the sharpness of the theoretically predicted waterfall in Fig. 1(c) is less severe than in experiments, which may be due to limitations of our model, including the approximations underlying our treatment of the susceptibility. On the other hand, the experimental situation remains somewhat unclear, and it has been suggested that matrix element effects could play a role in enhancing the apparent steepness of the waterfall.[25]

C. Electron doping

Figure 2 considers the case of electron-doped (overdoped) NCCO. The peak in Σ' in Fig. 2(a) lies at binding energies of 0.5–0.6 eV (in different $\vec{k}$ directions) with a height of 0.55–0.7 eV. Correspondingly, the peak in Σ'' in Fig. 2(b) lies at a binding energy of 0.7–1.1 eV with a height of 1–1.4 eV. Comparing these with the results of Fig. 1, we see that the self-energy effects in NCCO are much larger than in Bi2201. Our computed shift of ~300 meV in the position of the peak in Σ' to higher binding energy in going from Bi2201 to NCCO is in good accord with the experimentally reported shift of ~300 meV.[6,26] The dispersion underlying the dressed Green function, which may be tracked through the yellow dots, is highly anomalous and presents a kinklike feature quite reminiscent of the more familiar low-energy kinks in the 50 meV range around the $(\pi,0)$ direction,[27] which have been discussed frequently in the cuprates. This strong bosonic coupling is also reflected in the fact that the band bottom in NCCO lies several hundred meVs below the bare LDA band in Fig. 2(c). It is interesting to note that the self-energies of Figs. 1 and 2 display a "mirrorlike" symmetry: The peaks below the Fermi energy in Σ' and Σ'' for Bi2201 in Fig. 1 are smaller than those above the Fermi energy, but the situation reverses itself for NCCO in Fig. 2 in that now the peaks below the Fermi energy become larger than those above the Fermi energy.

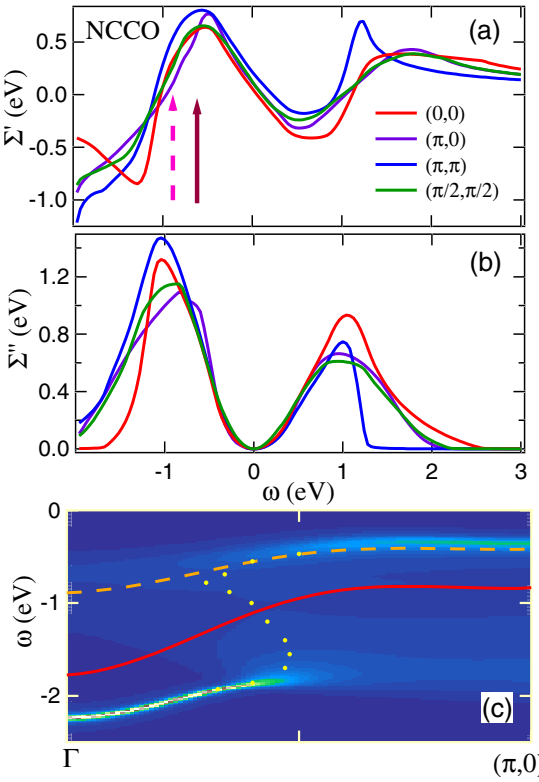

FIG. 2. (Color online) Same as Fig. 1, except that this figure shows only the computed results for overdoped NCCO. Experimental self-energies are not available and are therefore not shown (see text). The solid (dashed) arrow in (a) shows the location of the peak in χ'' at $(\pi,0)$ $[(\pi/2,\pi/2)]$.

III. RENORMALIZED SUSCEPTIBILITY

The aforementioned shift of the peak in Σ' to higher energy in NCCO can be understood in terms of the characteristics of the magnetic susceptibility. Figure 3 compares in Bi2201 and NCCO the imaginary part χ'', which is seen from Eq. (4) to be related directly to the real as well as the imaginary part of the self-energy. χ'' is seen to be quite similar in shape along the Γ to $(\pi,0)$ line in Bi2201 and NCCO, except that in NCCO the band of high intensity (the yellowish trace) extends to a significantly higher energy scale. In contrast, χ'' in the two systems differs sharply around (π,π). These differences reflect those in the low-energy magnetic response of the two cuprates. NCCO with strong magnetic response around (π,π) is close to a nearly commensurate antiferromagnetic (AFM) instability, while Bi2201 is very incommensurate, with peaks shifted toward $(\pi,0)$. In fact, the high-energy peaks in the self-energy in Figs. 1 and 2 are tied to the flat tops near $(\pi,0)$ at $\omega_1 \sim 0.36$ eV in Bi2201 (solid arrow), and near both $(\pi,0)$ at $\omega_2=0.62$ eV (solid arrow) and $(\pi/2,\pi/2)$ at $\omega_3=0.9$ eV (dashed arrow) in NCCO. Above these energies, the weight in χ'' falls rapidly, going to zero near an energy $8\bar{t}$.

A reference to Figs. 1(a) and 2(a), where the energy ω_1 in Bi2201, and the energies ω_2 and ω_3 in NCCO are marked by arrows, indicates that the peaks in Σ' are correlated with these features in the magnetic susceptibility. In this spirit, the

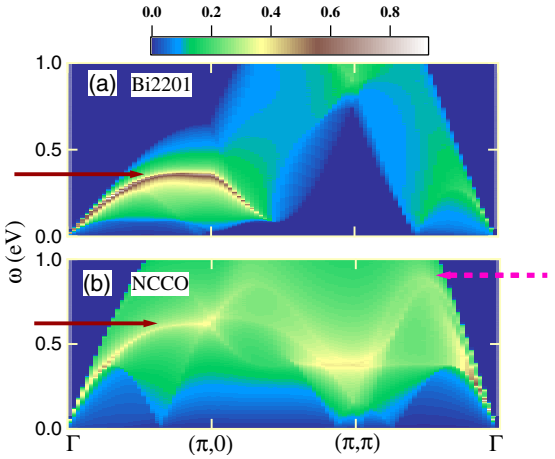

FIG. 3. (Color online) Map of the imaginary part of the magnetic susceptibility for (a) hole-doped Bi2201 and (b) electron-doped NCCO. Spectral weights are in units of eV^{-1}. Arrows mark the positions of the high spectral weights discussed in the text.

shift in the peak in Σ' to higher energy in going from Bi2201 to NCCO reflects the fact that feature ω_3 in χ'' at $(\pi/2,\pi/2)$ in NCCO [dashed arrow in Fig. 2(a)] lies at a higher energy than the $(\pi,0)$ feature ω_1 in Bi2201 [arrow in Fig. 1(a)]. Notably, when the generalized Stoner factor[28] $S_q=1/(1-U\chi_{0q})$ is large, a peak in χ'' arises from a peak in $\chi_0'(\omega)$, which in turn is associated with nesting of features separated by ω in energy. In the present case, the nesting is from unoccupied states near the Van Hove singularity (VHS) at $(\pi,0)$ to the vicinity of the band bottom at Γ, so $\omega_1 \sim 2(t+2t') \sim 0.32$ eV in Bi2201. The larger value of ω_2 in NCCO reflects the shift of the Fermi energy to higher energies in an electron-doped material.

IV. ELECTRON-ELECTRON SCATTERING

A notable difference between electron and hole doping is the low-ω behavior of Σ'', which is quadratic in ω for electron doping in Fig. 2(b), but nearly linear for hole doping in Fig. 1(b). The linearity for hole doping, reminiscent of marginal Fermi liquid physics, is associated here with the proximity of the chemical potential to the VHS. This point is considered further in Fig. 4, where Σ'' is shown in Bi2201 at the $(\pi,0)$ point for three different values of the chemical potential. When the chemical potential lies at the VHS (red line), Σ'' varies linearly, but when it is shifted by 75 meV above or below the VHS, the behavior changes rapidly to become parabolic.

The strong magnetic scattering discussed in this study in the case of overdoped cuprates should persist into the underdoped regime, where the generalized Stoner factor is expected to become larger. In fact, this scattering is a *precursor* to the antiferromagnetically ordered state near half-filling and it is responsible for opening the magnetic gap. In contrast, a number of authors have related the presence of waterfall-like effects near half-filling to "Mott" physics associated with (π,π) AFM fluctuations,[29–31] but have difficulty explaining why these effects persist into the overdoped regime.

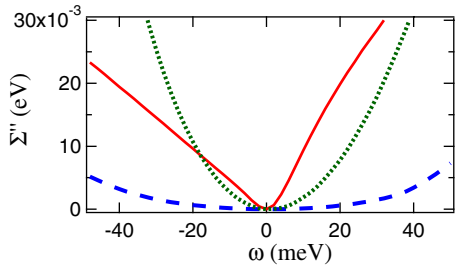

FIG. 4. (Color online) Low-energy behavior of $\Sigma''(\omega)$ at $(\pi,0)$ in Bi2201 for three different values of the chemical potential μ in relation to the position of the energy E_{VHS} of the Van Hove singularity. $E_{VHS}-\mu=0$ (red solid line), $E_{VHS}-\mu=+75$ meV (green dotted line), and $E_{VHS}-\mu=-75$ meV (blue dashed line).

V. CONCLUSIONS

The possible doping dependence of the *effective U* has been an important issue in connection with electron-doped cuprates. A doping-dependent U is suggested by a number of studies in the hole-doped cuprates as well. These include optical evidence of Mott gap decrease,[32] ARPES observation of LDA-like bands in optimally and overdoped materials, models of the magnetic resonance peak,[33] and, a strongly doping-dependent gap derived from Hall effect studies.[34] The $\bar{Z}^2$ renormalization of χ_0 in Eq. (2) bears on this question and gives insight into how the value of U enters into the magnetic response of the system. Recall that the susceptibility is often evaluated in the literature via Eq. (3) using experimental band parameters, but without the $\bar{Z}^2$ factor of Eq. (2) in χ_0, which yields a χ scaling $\sim\bar{Z}^{-1}$ rather than the correct scaling of $\chi\sim\bar{Z}$. This can be corrected by replacing the U in the Stoner factor by

$$U_{eff}=\bar{Z}^2U. \tag{5}$$

Indeed, our Hubbard parameter for NCCO of $U=4t$ is closer to the value at half-filling than is generally found.[35] A doping-dependent U (associated with vertex corrections) has recently been confirmed by Monte Carlo calculations of the Hubbard model.[36,37]

In conclusion, we have shown that the higher energy magnetic susceptibility in the cuprates has considerable weight near $(\pi,0)$ and that this leads to a high-energy kink or waterfall-like effect in dispersion in both electron- and hole-doped cuprates, providing an explanation of such effects observed recently in ARPES. Although our analysis is limited to the overdoped regime, we expect strong magnetic scattering to persist into the underdoped regime. This point, however, needs further study.

Note added. Recently, we became aware of two other calculations which adduce a similar origin for the waterfall effect. Macridin *et al.*[38] discussed a quantum Monte Carlo calculation for doped cuprates,[38] while Srivastava *et al.* considered the insulating phase.[39]

ACKNOWLEDGMENTS

This work is supported by the U.S. Department of Energy Contracts No. DE-AC03-76SF00098 and No. DE-FG02-07ER46352, and benefited from the allocation of supercomputer time at NERSC and Northeastern University's Advanced Scientific Computation Center (ASCC).

[1] F. Ronning, K. M. Shen, N. P. Armitage, A. Damascelli, D. H. Lu, Z.-X. Shen, L. L. Miller, and C. Kim, Phys. Rev. B **71**, 094518 (2005).
[2] J. Graf *et al.*, Phys. Rev. Lett. **98**, 067004 (2007).
[3] W. Meevasana *et al.*, Phys. Rev. B **75**, 174506 (2007).
[4] B. P. Xie *et al.*, Phys. Rev. Lett. **98**, 147001 (2007).
[5] T. Valla, T. E. Kidd, W.-G. Yin, G. D. Gu, P. D. Johnson, Z.-H. Pan, and A. V. Fedorov, Phys. Rev. Lett. **98**, 167003 (2007).
[6] Z.-H. Pan *et al.*, arXiv:cond-mat/0610442 (unpublished).
[7] J. Hwang, E. J. Nicol, T. Timusk, A. Knigavko, and J. P. Carbotte, Phys. Rev. Lett. **98**, 207002 (2007).
[8] A. Lanzara *et al.*, Nature (London) **412**, 510 (2001); X. J. Zhou *et al.*, Phys. Rev. Lett. **95**, 117001 (2005).
[9] A. Kaminski, M. Randeria, J. C. Campuzano, M. R. Norman, H. Fretwell, J. Mesot, T. Sato, T. Takahashi, and K. Kadowaki, Phys. Rev. Lett. **86**, 1070 (2001); P. D. Johnson *et al.*, *ibid.* **87**, 177007 (2001); S. V. Borisenko, A. A. Kordyuk, T. K. Kim, A. Koitzsch, M. Knupfer, M. S. Golden, J. Fink, M. Eschrig, H. Berger, and R. Follath, *ibid.* **90**, 207001 (2003); A. D. Gromko, A. V. Fedorov, Y.-D. Chuang, J. D. Koralek, Y. Aiura, Y. Yamaguchi, K. Oka, Y. Ando, and D. S. Dessau, Phys. Rev. B **68**, 174520 (2003).
[10] N. Nücker, H. Romberg, S. Nakai, B. Scheerer, J. Fink, Y. F. Yan, and Z. X. Zhao, Phys. Rev. B **39**, 12379 (1989).
[11] Y. Y. Wang, F. C. Zhang, V. P. Dravid, K. K. Ng, M. V. Klein, S. E. Schnatterly, and L. L. Miller, Phys. Rev. Lett. **77**, 1809 (1996).
[12] R. S. Markiewicz and A. Bansil, Phys. Rev. B **75**, 020508(R) (2007).
[13] K. McElroy *et al.*, Bull. Am. Phys. Soc. **51**, 141 (2006).
[14] Although not discussed here, we find similar results in LSCO.
[15] R. S. Markiewicz, S. Sahrakorpi, M. Lindroos, Hsin Lin, and A. Bansil, Phys. Rev. B **72**, 054519 (2005).
[16] For Bi2201, we use the parameters of $Bi_2Sr_2CaCu_2O_8$ (Bi2212), but neglect the bilayer splitting. Following Ref. 15, the hopping parameters are $(t,t',t'',t''')=(360,-100,35,10)$ meV for Bi2201 and $(420,-100,65,7.5)$ meV for NCCO.
[17] W. F. Brinkman and S. Engelsberg, Phys. Rev. **169**, 417 (1968).
[18] The specific values of Z are 0.28 in Bi2212 and 0.55 in NCCO (Ref. 15).
[19] Full self-consistency would make this a generalization of the self-consistent Born approximation in that χ_0 also involves renormalized bands. However, that approximation violates a Ward identity (Ref. 20), a problem avoided by the present approximation.
[20] See Eqs. A26–A29 of Y. M. Vilk and A.-M. S. Tremblay, J. Phys. I **7**, 1309 (1997).

[21] Specifically, $\bar{Z}$ is the renormalization of the coherent part of the dispersion.
[22] A. Lanzara (private communication).
[23] We fit the near-Fermi-surface dispersion over $\Gamma \rightarrow (\pi,0) \rightarrow (\pi,\pi) \rightarrow \Gamma$ ($\sim$100 k points) to a Z-renormalized bare dispersion, then shift the chemical potential to keep the corresponding density fixed.
[24] A. Bansil and M. Lindroos, Phys. Rev. Lett. **83**, 5154 (1999); S. Sahrakorpi, M. Lindroos, R. S. Markiewicz, and A. Bansil, *ibid.* **95**, 157601 (2005); A. Bansil, M. Lindroos, S. Sahrakorpi and R. S. Markiewicz, New J. Phys. **7**, 140 (2005).
[25] D. S. Inosov *et al.*, arXiv:cond-mat/0703223 (unpublished).
[26] In contrast, a strong coupling calculation [M. M. Zemljic, P. Prelovsek, and T. Tohyama, arXiv:0706.1156 (unpublished)] finds a large residual Mott gap and very weak waterfall effects for electron-doped cuprates below the Fermi level.
[27] A. Kaminski, M. Randeria, J. C. Campuzano, M. R. Norman, H. Fretwell, J. Mesot, T. Sato, T. Takahashi, and K. Kadowaki, Phys. Rev. Lett. **86**, 1070 (2001).
[28] A. Auerbach, *Interacting Electrons and Quantum Magnetism* (Springer, New York, 1994), Eq. 4.25.
[29] Y. Kakehashi and P. Fulde, J. Phys. Soc. Jpn. **74**, 2397 (2005).
[30] E. Manousakis, Phys. Lett. A **362**, 86 (2007).
[31] Q.-H. Wang, F. Tan, and Y. Wan, Phys. Rev. B **76**, 054505 (2007).
[32] S. Uchida, T. Ido, H. Takagi, T. Arima, Y. Tokura, and S. Tajima, Phys. Rev. B **43**, 7942 (1991).
[33] H. Woo, Pengcheng Dai, S. M. Hayden, H. A. Mook, T. Dahm, D. J. Scalapino, T. G. Perring, and F. Dogan, Nat. Phys. **2**, 600 (2006).
[34] S. Ono, S. Komiya, and Y. Ando, Phys. Rev. B **75**, 024515 (2007). The stronger doping dependence may be due to the high measurement temperatures.
[35] The smaller U for Bi2201 may be due to neglect of the k_z dispersion, which broadens features in χ near the VHS.
[36] T. A. Maier, M. Jarrell, and D. J. Scalapino, Phys. Rev. B **75**, 134519 (2007).
[37] Z. B. Huang, W. Hanke, E. Arrigoni, and A. V. Chubukov, Phys. Rev. B **74**, 184508 (2006).
[38] A. Macridin, M. Jarrell, T. Maier, and D. J. Scalapino, arXiv:cond-mat/0701429 (unpublished).
[39] P. Srivastava, S. Ghosh, and A. Singh, arXiv:0707.2267 (unpublished).